Granular flow based on 3D DDA

Zeyang Wu(1), Changdong Liu(2), Zhongmin Mao(3)
China university of Geosciences
Wuhan, China

Instructor: Prof. Yuyong Jiao (yyjiao@cug.edu.cn)
Zeyang Wu ： 769148467@qq.com
Changdong Liu：liuchangdong@cug.edu.cn
Zhongmin Mao：maozhongmin@cug.edu.cn

Discontinuous deformation analysis (DDA) is an important numerical simulation method for solving the mechanical problems of discontinuous media, which can more realistically reproduce the damage process of materials. The three-dimensional sphere DDA (3D SDDA) is based on the block DDA, which simplifies the block units into spheres. In this paper, the self-made 3D SDDA program is used to simulate the collapse process of sand column. Firstly, the principle and data structure of the program are introduced, and then the relevant calculation parameters of the program are calibrated to predict the possible accumulation effect of sand column collapse of test 5 and 6 by comparing the simulation results with the experimental results.

Keywords: spherical discontinuous deformation analysis (SDDA);

I. Numerical methods and software (Heading 1)

The 3D SDDA program [1,2] developed by Jiao's team was used to simulate problem B. The calculation principle and programming method of 3D SDDA will be described in detail below.

1.1 The Basic Formulation of 3D SDDA

The three-dimensional sphere DDA (3D SDDA) is based on the block DDA [3], which simplifies the block units into spheres. It uses the sphere center coordinates and

sphere radius to describe the position of the sphere unit in 3D space. It simplifies the contact type of block unit from complex "edge-edge", "edge-angle" and "angle-angle" to " sphere-sphere" and " sphere-face and also simplifies the displacement and deformation of the unit in the system.

1.1.1 Energy Minimization and Equilibrium Equations

The dynamic mechanical response of the global particle system in a certain period can be solved by minimizing the total potential energy of the system, where the kinetic energy terms is integrated by the constant acceleration-based Newmark integration approach. The global equilibrium equation in an analysis step can be obtained as follows:

$$\begin{bmatrix} \mathbf{K}_{11} & \mathbf{K}_{12} & \mathbf{K}_{13} & \cdots & \mathbf{K}_{1n} \\ \mathbf{K}_{21} & \mathbf{K}_{22} & \mathbf{K}_{23} & \cdots & \mathbf{K}_{2n} \\ \mathbf{K}_{31} & \mathbf{K}_{32} & \mathbf{K}_{33} & \cdots & \mathbf{K}_{3n} \\ \vdots & \vdots & \vdots & \ddots & \vdots \\ \mathbf{K}_{n1} & \mathbf{K}_{n2} & \mathbf{K}_{n3} & \cdots & \mathbf{K}_{nn} \end{bmatrix} \begin{bmatrix} \mathbf{d}_1 \\ \mathbf{d}_2 \\ \mathbf{d}_3 \\ \vdots \\ \mathbf{d}_n \end{bmatrix} = \begin{bmatrix} \mathbf{f}_1 \\ \mathbf{f}_2 \\ \mathbf{f}_3 \\ \vdots \\ \mathbf{f}_n \end{bmatrix} \tag{1}$$

where $\mathbf{K}_{ii}$ represent the diagonal 6×6 sub-matrix for sphere i; $\mathbf{K}_{ij}(i \neq j)$ represent a 6×6 off-diagonal sub-matrix with respect to contact spheres i and j; $\mathbf{d}_i$ represent the incremental DOF values of the i^{th} sphere; $\mathbf{f}_i$ represent the force vectors acting on the i^{th} sphere.

In the SDDA method, spherical shape is used to simplify the complex contact geometry of polyhedral blocks. In addition, each sphere is assumed to be rigid to decrease the total degree of freedom (DOF) in a large model. The displacement $\mathbf{u}_p = \begin{bmatrix} u_p & v_p & w_p \end{bmatrix}^T$ of a point $p(x_p, y_p, z_p)$ in a rigid sphere is computed by $\mathbf{u}_p = \mathbf{T}_{(x_p,y_p,z_p)}\mathbf{d}$, where $\mathbf{T}_{(x_p,y_p,z_p)}$ is the 3×6 matrix of shape function and is the DOF vector of the rigid sphere.

1.1.2 Displacement and Deformation of Sphere

In the 3D SDDA method, each sphere is assumed to be rigid to decrease the total degree of freedom in a large model. Therefore, the displacement and deformation of the

sphere are defined by six degrees of freedom as follow:

$$\mathbf{d} = \begin{bmatrix} d_x & d_y & d_z & r_x & r_y & r_z \end{bmatrix}^T \tag{2}$$

where $\mathbf{d}_i$ represent the displacements along the x-, the y- and the z-axes, and r_i represent the rotation angles around the sphere center.

The displacement function of an arbitrary point (x, y, z) of sphere *i* can be written as:

$$\begin{bmatrix} u_p & v_p & w_p \end{bmatrix}^T = [\mathbf{T}_i(x, y, z)\mathbf{d}] \tag{3}$$

where $\mathbf{T}_i(x, y, z)$ is called the displacement transformation matrix of sphere *i*,

$$\mathbf{T}_i(x, y, z) = \begin{pmatrix} 1 & 0 & 0 & 0 & \bar{z} & -\bar{y} \\ 0 & 1 & 0 & -\bar{z} & 0 & \bar{x} \\ 0 & 0 & 1 & \bar{y} & -\bar{x} & 0 \end{pmatrix} \tag{4}$$

where $\bar{x} = x - x_c$, $\bar{y} = y - y_c$, $\bar{z} = z - z_c$ and (x_c, y_c, z_c) are the coordinates of the center of sphere *i*.

1.1.3 Submatrix of Initial Stress

The potential energy of sphere *I* is

$$\begin{aligned} \Pi_I &= -\iiint [\begin{bmatrix} u_p & v_p & w_p \end{bmatrix}][\begin{matrix} f_x & f_y & f_z \end{matrix}]^T dxdydz \\ &= \iiint \rho [D_i]^T [T_i(x, y, z)]^T [T_i(x, y, z)] \frac{\partial^2}{\partial t^2} [D_i(t)] dxdydz \\ &= \rho [D_i]^T \iiint [T_i(x, y, z)]^T [T_i(x, y, z)] dxdydz (\frac{2}{\Delta^2} [D_i] - \frac{2}{\Delta} [V_i(0)]) \end{aligned} \tag{5}$$

By minimizing $\prod_I$, initial stress submatrices of sphere *i* are obtained

$$\begin{aligned} &\frac{2\rho}{\Delta^2} \iiint [T_i(x, y, z)]^T [T_i(x, y, z)] dxdydz \to [K_{ii}] \\ &\frac{2\rho}{\Delta} \iiint [T_i(x, y, z)]^T [T_i(x, y, z)] dxdydz [V_i(0)] \to [F_i] \end{aligned} \tag{6}$$

1.1.4 Submatrix of sphere-sphere contact

As show in Fig. 1, the spheres *i* and *j* come into contact in the next step, and the radii of the two spheres are R_i and R_j respectively. The centers of the two spheres are $C_i(x_{Ci}, y_{Ci}, z_{Ci})$ and $C_j(x_{Cj}, y_{Cj}, z_{Cj})$ respectively.

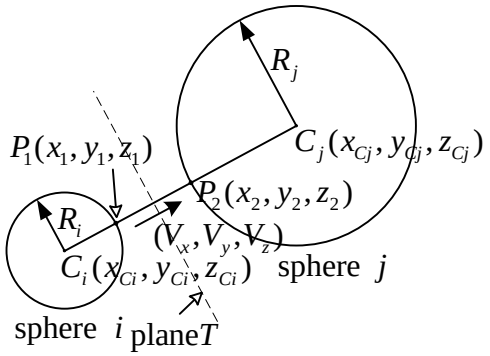

Fig. 1 sphere-sphere contact.

The unit vector of $\overrightarrow{C_iC_j}$ is (V_x, V_y, V_z). If the $P_1(x_1, y_1, z_1)$ of sphere *i* is in contact with $P_2(x_2, y_2, z_2)$ of sphere *j*, the values of the coordinates of the two points are

$$P_1: \begin{cases} x_1 = x_{Ci} + V_x R_i \\ y_1 = y_{Ci} + V_y R_i \\ z_1 = z_{Ci} + V_z R_i \end{cases} \tag{7}$$

$$P_2: \begin{cases} x_2 = x_{Cj} - V_x R_j \\ y_2 = y_{Cj} - V_y R_j \\ z_2 = z_{Cj} - V_z R_j \end{cases} \tag{8}$$

The displacements of P_1 and P_2 are (u_1, v_1, w_1) and (u_2, v_2, w_2), and the distance between P_1 and P_2 can be get by follow formula.

$$d^2 = \begin{bmatrix} (x_2 + u_2) - (x_1 + u_1) \\ (y_2 + v_2) - (y_1 + v_1) \\ (z_2 + w_2) - (z_1 + w_1) \end{bmatrix}^T \begin{bmatrix} (x_2 + u_2) - (x_1 + u_1) \\ (y_2 + v_2) - (y_1 + v_1) \\ (z_2 + w_2) - (z_1 + w_1) \end{bmatrix}$$

$$= \begin{bmatrix} (x_2 - x_1) + (u_2 - u_1) \\ (y_2 - y_1) + (v_2 - v_1) \\ (z_2 - z_1) + (w_2 - w_1) \end{bmatrix}^T \begin{bmatrix} (x_2 - x_1) + (u_2 - u_1) \\ (y_2 - y_1) + (v_2 - v_1) \\ (z_2 - z_1) + (w_2 - w_1) \end{bmatrix}$$

$$= \left(\begin{bmatrix} x_2 - x_1 \\ y_2 - y_1 \\ z_2 - z_1 \end{bmatrix}^T + [D_j]^T [T_j(x_2, y_2, z_2)]^T - [D_i]^T [T_i(x_1, y_1, z_1)]^T \right)$$

$$\left(\begin{bmatrix} x_2 - x_1 \\ y_2 - y_1 \\ z_2 - z_1 \end{bmatrix} + [T_j(x_2, y_2, z_2)][D_j] - [T_i(x_1, y_1, z_1)][D_i] \right) \tag{9}$$

$$d^2 = \begin{bmatrix} x_2 - x_1 \\ y_2 - y_1 \\ z_2 - z_1 \end{bmatrix}^T \begin{bmatrix} x_2 - x_1 \\ y_2 - y_1 \\ z_2 - z_1 \end{bmatrix} - 2[D_j]^T [T_j(x_2, y_2, z_2)]^T [T_i(x_1, y_1, z_1)][D_i]$$

$$+ 2[D_j]^T [T_j(x_2, y_2, z_2)]^T \begin{bmatrix} x_2 - x_1 \\ y_2 - y_1 \\ z_2 - z_1 \end{bmatrix} - 2[D_i]^T [T_i(x_1, y_1, z_1)]^T \begin{bmatrix} x_2 - x_1 \\ y_2 - y_1 \\ z_2 - z_1 \end{bmatrix}$$

$$+ [D_j]^T [T_j(x_2, y_2, z_2)]^T [T_j(x_2, y_2, z_2)][D_j]$$

$$+ [D_i]^T [T_i(x_1, y_1, z_1)]^T [T_i(x_1, y_1, z_1)][D_i] \tag{10}$$

The normal distance d_N between sphere *i* and sphere *j* is

$$d_N = \begin{bmatrix} V_x \\ V_y \\ V_z \end{bmatrix}^T \begin{bmatrix} (x_2 - x_1) + (u_2 - u_1) \\ (y_2 - y_1) + (v_2 - v_1) \\ (z_2 - z_1) + (w_2 - w_1) \end{bmatrix} = \begin{bmatrix} V_x \\ V_y \\ V_z \end{bmatrix}^T \begin{bmatrix} u_2 - u_1 \\ v_2 - v_1 \\ w_2 - w_1 \end{bmatrix} + \delta \tag{11}$$

and

$$\delta = \begin{bmatrix} V_x \\ V_y \\ V_z \end{bmatrix}^T \begin{bmatrix} x_2 - x_1 \\ y_2 - y_1 \\ z_2 - z_1 \end{bmatrix} \tag{12}$$

The potential energy of the normal spring between sphere *i* and sphere *j* is

$$\Pi_{N1} = \frac{p_N}{2} d_N^2 = \frac{p_N}{2} \left(\begin{bmatrix} u_2 - u_1 \\ v_2 - v_1 \\ w_2 - w_1 \end{bmatrix}^T \begin{bmatrix} V_x \\ V_y \\ V_z \end{bmatrix} + \delta \right) \left(\begin{bmatrix} V_x \\ V_y \\ V_z \end{bmatrix}^T \begin{bmatrix} u_2 - u_1 \\ v_2 - v_1 \\ w_2 - w_1 \end{bmatrix} + \delta \right)$$

$$= \frac{p_N}{2} \left(\begin{bmatrix} u_2 \\ v_2 \\ w_2 \end{bmatrix}^T \begin{bmatrix} V_x \\ V_y \\ V_z \end{bmatrix} - \begin{bmatrix} u_1 \\ v_1 \\ w_1 \end{bmatrix}^T \begin{bmatrix} V_x \\ V_y \\ V_z \end{bmatrix} + \delta \right) \left(\begin{bmatrix} V_x \\ V_y \\ V_z \end{bmatrix}^T \begin{bmatrix} u_2 \\ v_2 \\ w_2 \end{bmatrix} - \begin{bmatrix} V_x \\ V_y \\ V_z \end{bmatrix}^T \begin{bmatrix} u_1 \\ v_1 \\ w_1 \end{bmatrix} + \delta \right) \tag{13}$$

and $\begin{bmatrix} u_1 \\ v_1 \\ w_1 \end{bmatrix}^T \begin{bmatrix} V_x \\ V_y \\ V_z \end{bmatrix} = [D_i]^T [T_i(x_1, y_1, z_1)]^T \begin{bmatrix} V_x \\ V_y \\ V_z \end{bmatrix}$

$$= [D_i]^T \begin{bmatrix} 1 & 0 & 0 & 0 & V_z R_i & -V_y R_i \\ 0 & 1 & 0 & -V_z R_i & 0 & V_x R_i \\ 0 & 0 & 1 & V_y R_i & -V_x R_i & 0 \end{bmatrix}^T \begin{bmatrix} V_x \\ V_y \\ V_z \end{bmatrix}$$

$$= [D_i]^T [V_x \quad V_y \quad V_z \quad 0 \quad 0 \quad 0]^T = [D_i]^T [V_N]^T \tag{14}$$

By combining the above equations,

$$\Pi_{N1} = \frac{p_N}{2} \delta^2 + \frac{p_N}{2} [D_j]^T [V_N]^T [V_N][D_j] + \frac{p_N}{2} [D_i]^T [V_N]^T [V_N][D_i]$$

$$+ p_N \delta [D_j]^T [V_N]^T - p_N \delta [D_i]^T [V_N]^T - p_N [D_i]^T [V_N]^T [V_N][D_j] \tag{15}$$

By minimizing Π_{N1}, normal contact submatrices of sphere *i* and sphere *j* are obtained:

$$p_N [V_N]^T [V_N] \rightarrow [K_{ii}] \tag{16}$$

$$- p_N [V_N]^T [V_N] \rightarrow [K_{ij}] \tag{17}$$

$$- p_N [V_N]^T [V_N] \rightarrow [K_{ji}] \tag{18}$$

$$p_N [V_N]^T [V_N] \rightarrow [K_{jj}] \tag{19}$$

$$p_N \delta [V_N]^T \rightarrow [F_i] \tag{20}$$

$$- p_N \delta [V_N]^T \rightarrow [F_j] \tag{21}$$

The potential energy of the shear spring between sphere *i* and sphere *j* is

$$\Pi_{S1} = \frac{p_S}{2} d_S^2 = \frac{p_S}{2} d^2 - \frac{p_S}{2} d_N^2 \tag{22}$$

$$\Pi_{S1} = \frac{p_S}{2} \begin{bmatrix} x_2 - x_1 \\ y_2 - y_1 \\ z_2 - z_1 \end{bmatrix}^T \begin{bmatrix} x_2 - x_1 \\ y_2 - y_1 \\ z_2 - z_1 \end{bmatrix} - p_S [D_j]^T [T_j(x_2, y_2, z_2)]^T [T_i(x_1, y_1, z_1)][D_i]$$

$$+ p_S[D_j]^T[T_j(x_2,y_2,z_2)]^T\begin{bmatrix}x_2-x_1\\y_2-y_1\\z_2-z_1\end{bmatrix} - p_S[D_i]^T[T_i(x_1,y_1,z_1)]^T\begin{bmatrix}x_2-x_1\\y_2-y_1\\z_2-z_1\end{bmatrix}$$

$$+ \frac{p_S}{2}[D_j]^T[T_j(x_2,y_2,z_2)]^T[T_j(x_2,y_2,z_2)][D_j]$$

$$+ \frac{p_S}{2}[D_i]^T[T_i(x_1,y_1,z_1)]^T[T_i(x_1,y_1,z_1)][D_i]$$

$$-\frac{p_N}{2}\delta^2 - \frac{p_N}{2}[D_j]^T[V_N]^T[V_N][D_j] - \frac{p_N}{2}[D_i]^T[V_N]^T[V_N][D_i]$$

$$- p_N\delta[D_j]^T[V_N]^T + p_N\delta[D_i]^T[V_N]^T + p_N[D_i]^T[V_N]^T[V_N][D_j] \tag{23}$$

By minimizing $\prod_{S1}$, shear contact submatrices of sphere *i* and sphere *j* are obtained:

$$p_S[T_i(x_1,y_1,z_1)]^T[T_i(x_1,y_1,z_1)] - p_S[V_N]^T[V_N] \to [K_{ii}] \tag{24}$$

$$- p_S[T_i(x_1,y_1,z_1)]^T[T_j(x_2,y_2,z_2)] + p_S[V_N]^T[V_N] \to [K_{ij}] \tag{25}$$

$$- p_S[T_j(x_2,y_2,z_2)]^T[T_i(x_1,y_1,z_1)] + p_S[V_N]^T[V_N] \to [K_{ji}] \tag{26}$$

$$p_S[T_j(x_2,y_2,z_2)]^T[T_j(x_2,y_2,z_2)] - p_S[V_N]^T[V_N] \to [K_{jj}] \tag{27}$$

$$p_S[T_i(x_1,y_1,z_1)]^T\begin{bmatrix}x_2-x_1\\y_2-y_1\\z_2-z_1\end{bmatrix} - p_S\delta[V_N]^T \to [F_i] \tag{28}$$

$$- p_S[T_j(x_2,y_2,z_2)]^T\begin{bmatrix}x_2-x_1\\y_2-y_1\\z_2-z_1\end{bmatrix} + p_S\delta[V_N]^T \to [F_j] \tag{29}$$

Assuming that at the end of the time step P_1 and P_2 move to points P_1* and P_2*, respectively. The unit vector of $\overrightarrow{P_1*P_2*}$ is (l,m,n), then the potential energy of the friction force between sphere *i* and sphere *j* can be obtained as follow:

$$\Pi_{f1} = f_S([u_2 \quad v_2 \quad w_2] - [u_1 \quad v_1 \quad w_1])[l \quad m \quad n]^T$$

$$= f_S([D_j]^T[T_j(x_2,y_2,z_2)]^T - [D_i]^T[T_i(x_1,y_1,z_1)]^T)[l \quad m \quad n]^T \tag{30}$$

By minimizing $\prod_{f1}$, friction force submatrices of sphere *i* and sphere *j* are obtained:

$$f_S[T_i(x_1,y_1,z_1)]^T[l \quad m \quad n]^T \to [F_i] \tag{31}$$

$$-f_S[T_j(x_2,y_2,z_2)]^T[l \quad m \quad n]^T \to [F_j] \tag{32}$$

1.1.5 Submatrix of sphere-face contact

As show in Fig.2, the sphere *i* and face *F* come into contact in the next step, and the $P_1(x_1,y_1,z_1)$ of sphere *i* is in contact with $P_2(x_2,y_2,z_2)$ of face *F*. The unit vector of $\overrightarrow{C_iP_2}$ is (V_x,V_y,V_z).

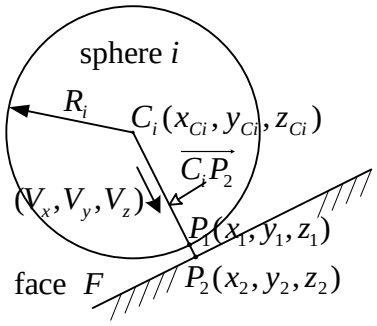

Fig. 2 sphere-face contact.

The displacements of P_1 is (u_1,v_1,w_1), and the distance between P_1 and P_2 can be get by follow formula.

$$d^2 = \begin{bmatrix} x_2-(x_1+u_1) \\ y_2-(y_1+v_1) \\ z_2-(z_1+w_1) \end{bmatrix}^T \begin{bmatrix} x_2-(x_1+u_1) \\ y_2-(y_1+v_1) \\ z_2-(z_1+w_1) \end{bmatrix}$$

$$= (\begin{bmatrix} x_2-x_1 \\ y_2-y_1 \\ z_2-z_1 \end{bmatrix}^T - [D_i]^T[T_i(x_1,y_1,z_1)]^T)(\begin{bmatrix} x_2-x_1 \\ y_2-y_1 \\ z_2-z_1 \end{bmatrix} - [T_i(x_1,y_1,z_1)][D_i])$$

$$= \begin{bmatrix} x_2-x_1 \\ y_2-y_1 \\ z_2-z_1 \end{bmatrix}^T \begin{bmatrix} x_2-x_1 \\ y_2-y_1 \\ z_2-z_1 \end{bmatrix} - 2[D_i]^T[T_i(x_1,y_1,z_1)]^T \begin{bmatrix} x_2-x_1 \\ y_2-y_1 \\ z_2-z_1 \end{bmatrix}$$

$$+[D_i]^T[T_i(x_1,y_1,z_1)]^T[T_i(x_1,y_1,z_1)][D_i] \tag{33}$$

The normal distance d_N between sphere *i* and face *F* is

$$d_N=\begin{bmatrix}V_x\\V_y\\V_z\end{bmatrix}^T\begin{bmatrix}x_2-(x_1+u_1)\\y_2-(y_1+v_1)\\z_2-(z_1+w_1)\end{bmatrix}=\lambda-\begin{bmatrix}V_x\\V_y\\V_z\end{bmatrix}^T\begin{bmatrix}u_1\\v_1\\w_1\end{bmatrix} \tag{34}$$

and

$$\lambda=\begin{bmatrix}V_x\\V_y\\V_z\end{bmatrix}^T\begin{bmatrix}x_2-x_1\\y_2-y_1\\z_2-z_1\end{bmatrix} \tag{35}$$

The potential energy of the normal spring between sphere *i* and face *F* is

$$\Pi_{N2}=\frac{p_N}{2}d_N^2=\frac{p_N}{2}(\lambda-\begin{bmatrix}u_1\\v_1\\w_1\end{bmatrix}^T\begin{bmatrix}V_x\\V_y\\V_z\end{bmatrix})(\lambda-\begin{bmatrix}V_x\\V_y\\V_z\end{bmatrix}^T\begin{bmatrix}u_1\\v_1\\w_1\end{bmatrix})$$

$$=\frac{p_N}{2}\lambda^2-p_N\lambda\begin{bmatrix}u_1\\v_1\\w_1\end{bmatrix}^T\begin{bmatrix}V_x\\V_y\\V_z\end{bmatrix}+\frac{p_N}{2}\begin{bmatrix}u_1\\v_1\\w_1\end{bmatrix}^T\begin{bmatrix}V_x\\V_y\\V_z\end{bmatrix}\begin{bmatrix}V_x\\V_y\\V_z\end{bmatrix}^T\begin{bmatrix}u_1\\v_1\\w_1\end{bmatrix}$$

$$=\frac{p_N}{2}\lambda^2-p_N\lambda[D_i]^T[V_N]^T+\frac{p_N}{2}[D_i]^T[V_N]^T[V_N][D_i] \tag{36}$$

By minimizing Π_{N2}, normal contact submatrices of sphere *i* are

$$p_N[V_N]^T[V_N]\rightarrow[K_{ii}] \tag{37}$$

$$p_N\lambda[V_N]^T\rightarrow[F_i] \tag{38}$$

The potential energy of the shear spring between sphere *i* and face *F* is

$$\Pi_{S2}=\frac{p_S}{2}d_S^2=\frac{p_S}{2}d^2-\frac{p_S}{2}d_N^2$$

$$=\frac{p_S}{2}\begin{bmatrix}x_2-x_1\\y_2-y_1\\z_2-z_1\end{bmatrix}^T\begin{bmatrix}x_2-x_1\\y_2-y_1\\z_2-z_1\end{bmatrix}-p_S[D_i]^T[T_i(x_1,y_1,z_1)]^T\begin{bmatrix}x_2-x_1\\y_2-y_1\\z_2-z_1\end{bmatrix}$$

$$+\frac{p_S}{2}[D_i]^T[T_i(x_1,y_1,z_1)]^T[T_i(x_1,y_1,z_1)][D_i]$$

$$-\frac{p_S}{2}\lambda^2 + p_S\lambda[D_i]^T[V_N]^T - \frac{p_S}{2}[D_i]^T[V_N]^T[V_N][D_i] \tag{39}$$

By minimizing $\prod_{S2}$, shear contact submatrices of sphere *i* are obtained:

$$p_S[T_i(x_1, y_1, z_1)]^T[T_i(x_1, y_1, z_1)] - p_S[V_N]^T[V_N] \to [K_{ii}] \tag{40}$$

$$p_S[T_i(x_1, y_1, z_1)]^T\begin{bmatrix} x_2 - x_1 \\ y_2 - y_1 \\ z_2 - z_1 \end{bmatrix} - p_S\lambda[V_N]^T \to [F_i] \tag{41}$$

The formula for calculating the friction force between sphere *i* and face *F* is:

$$f_S = p_N d_P \tan\varphi \tag{42}$$

Assuming that at the end of the time-step P_1 move to points P_1*. The unit vector of $\overrightarrow{P_1*P_2*}$ is (l, m, n), then the potential energy of the friction force between sphere *i* and face *F* can be obtained as follow:

$$\Pi_{f2} = f_S[u_1 \quad v_1 \quad w_1][l \quad m \quad n]^T = f_S[D_i]^T[T_i(x_1, y_1, z_1)]^T[l \quad m \quad n]^T \tag{43}$$

By minimizing $\prod_{f2}$, friction force submatrices of sphere *i* is obtained:

$$-f_S[T_i(x_1, y_1, z_1)]^T[l \quad m \quad n]^T \to [F_i] \tag{44}$$

1.2 Software

The following will briefly introduce the self-made numerical software used in this modeling from the calculation process of 3D SDDA, program composition and C++ programming method.

The whole program includes three main modules, i.e., a preprocessor, an analysis module, and a postprocessor. Each module defines the relevant file interface for data transmission.

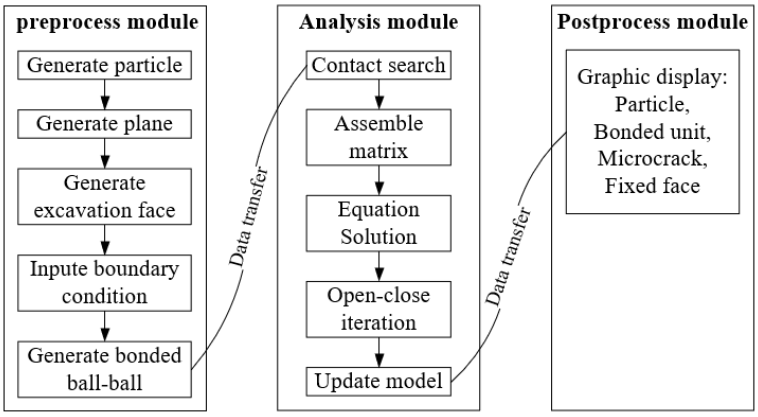

Fig. 3 program module.

1.2.1 Calculation Process

The flowchart of computation loops in 3D SDDA program is shown in Fig.4. The contact search is performed first, then the simultaneous equations are solved based on the contact pairs and other information, followed by open-closed iteration step to detecting the solution results, and finally the next cycle is calculated after increasing or decreasing the penalty spring or reducing the time step based on the detection results until the contact patterns of all contact pairs meet the requirements.

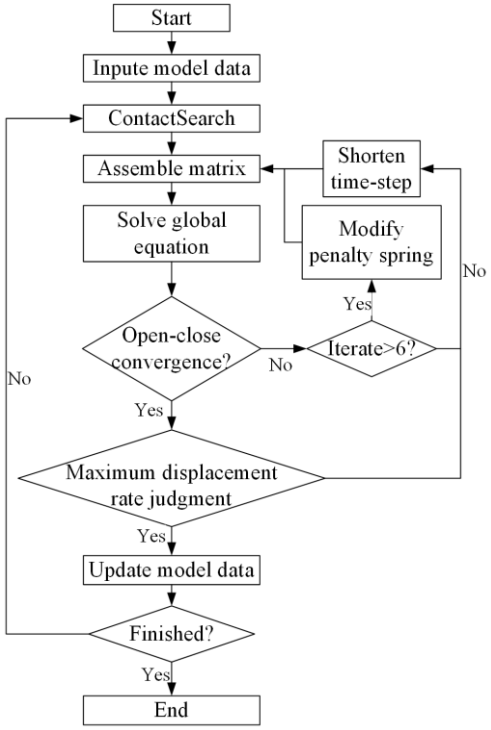

Fig. 4 Flowchart of computation loops in 3D SDDA program.

1.2.2 Data Structure

In order to improve the performance of the program, the following data structure is used in the calculation module. Class SDDA is the biggest class that adopts the objects of many small classes and calculation parameters. Class Ball is used to define the sphere in 3D space. The member variables of class Ball mainly include the physical information of the sphere and the relevant contact information.

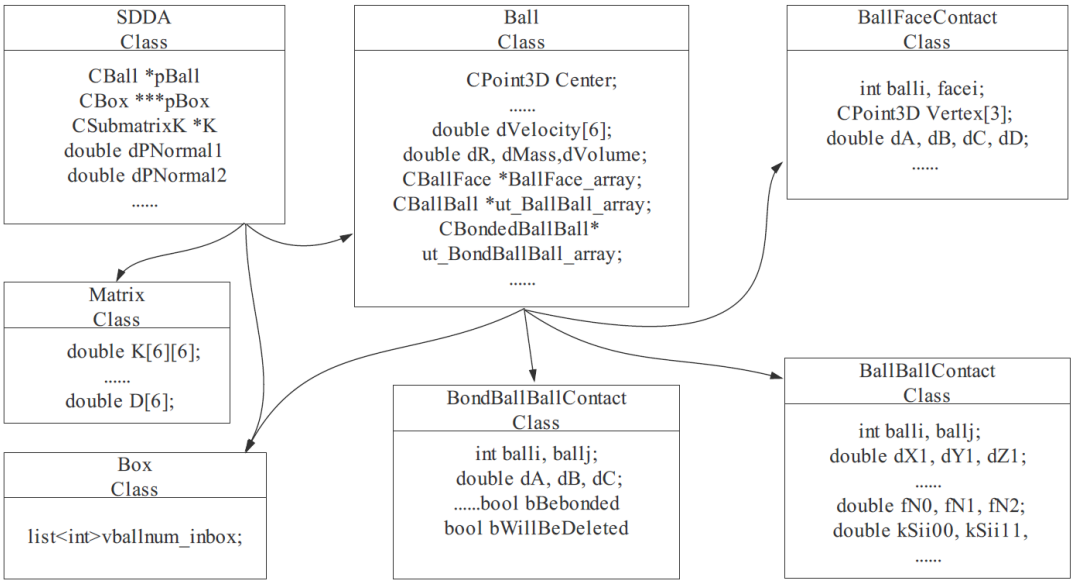

Fig. 5 Data structure of 3D SDDA.

II. Numerical modelling

The model of Test1-6 in question B is shown in the Fig.6, and the numerical models of corresponding sizes and boundary conditions are established according to the experimental results. In order to make the simulations more concise and efficient, equal diameter spheres are used in this simulation. The sphere accumulation pattern is body-centered cubic model shown in Fig.7, and the radius of sphere is 0.0069m, and the total number of spheres in each model are: 7428, 14412, 21756, 14412, 14412, 21756 respectively.

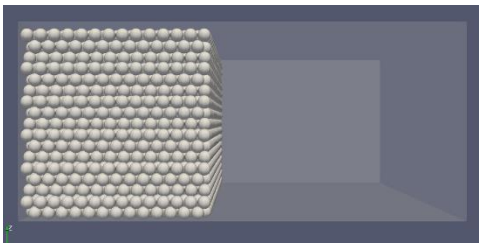

Fig. 6 Numerical model demonstration

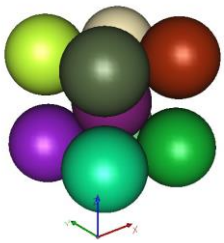

Fig. 7 Body-centered cubic model.

Firstly, the microscopic parameters of spheres were calibrated by simulating test 1-4 so that the experiment effect of tests 5-6 could be predicted by numerical simulation. The parameters to be calibrated mainly include: normal and shear contact spring stiffness, sphere-sphere friction angle sphere-face friction angle, sphere density, maximum displacement ratio and time step. The simulation error is calculated as follows:

$$\text{Error}=\left|L_t-L_s\right|/L_t*100\% \tag{45}$$

where, L_t is the experimental results, L_s is the simulation results.

III. Clabration results

In order to make the simulation results closer to the actual situation, four groups of models are built according to test1 to 4, and the microscopic parameters in the sphere system are calibrated. The final parameter calibration results are shown in Table 1

Table1 Computational mechanical parameters.

Parameter	Value
Density（kg/m^3）	2000
Ball-ball normal spring stiffness (GN/m)	1

Ball-ball shear spring stiffness (GN/m)	0.5
Ball-face normal spring stiffness (GN/m)	1
Ball-face shear spring stiffness (GN/m)	0.5
Sphere-sphere frictional angle	36°
Sphere-face frictional angle	10°
Time step	1e-5

3.1 Test 1

The size of sand column for test 1 is 20*40*20 (length*width*height). Table 2 shows the simulation results with the experimental results and the errors. The displacement results shown in Fig. 8 are basically consistent with the experimental results.

Table 2 Comparison of experimental and simulation results.

	Final deposit height (Hi)	Final deposit length (Li)	Inclination /°
Experiment result	20	40	29.5
Numerical result	20	41	30.5
Error (%)	0	2.5	3.4

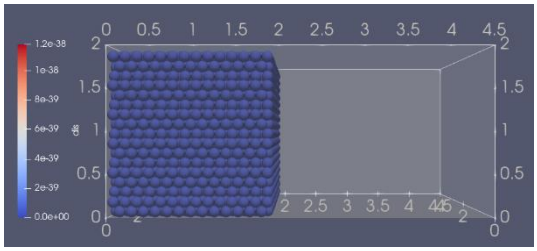

(a) time step=0

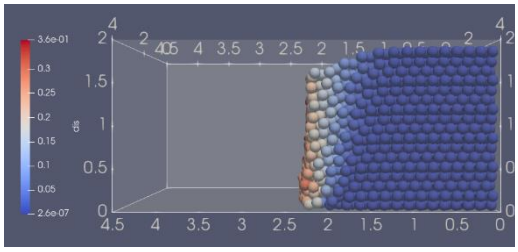

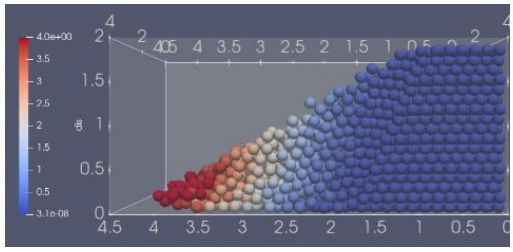

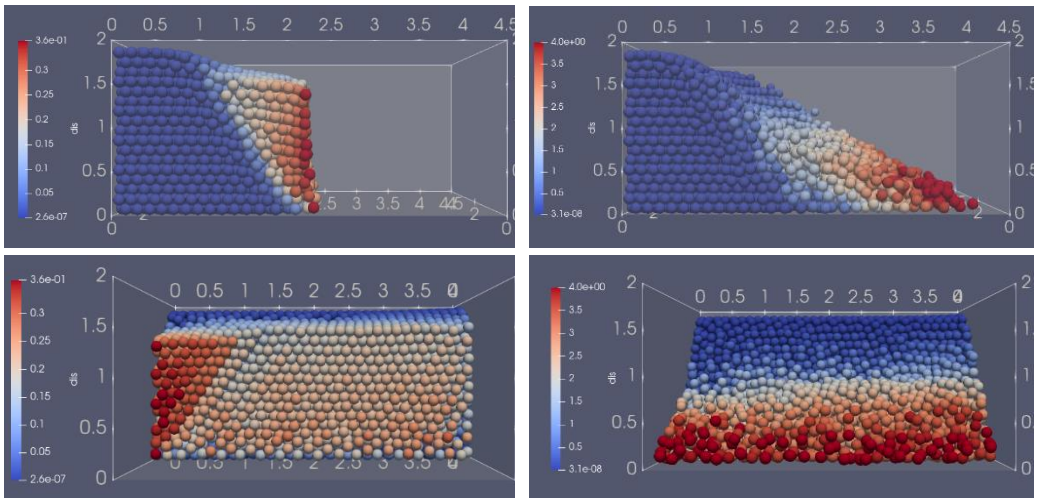

(b) time step=45,000 (c) time step=90,000

Fig. 8 Configurations of the initial model and the simulation results at 0, 45,000, 90,000 time steps.

3.2 Test 2

The size of sand column for test 2 is 20*40*40 (length*width*height). Table 3 shows the simulation results with the experimental results and the errors. The displacement results shown in Fig. 9 are basically consistent with the experimental results.

Table 3 Comparison of experimental and simulation results

	Final deposit height (Hi)	Final deposit length (Li)	Inclination /°
Experiment result	31	62	26.5
Numerical result	30	63	25.5
Error (%)	3.2	1.6	3.8

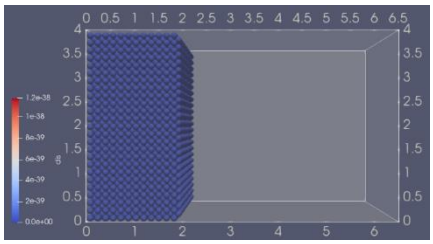

(a) time step=0

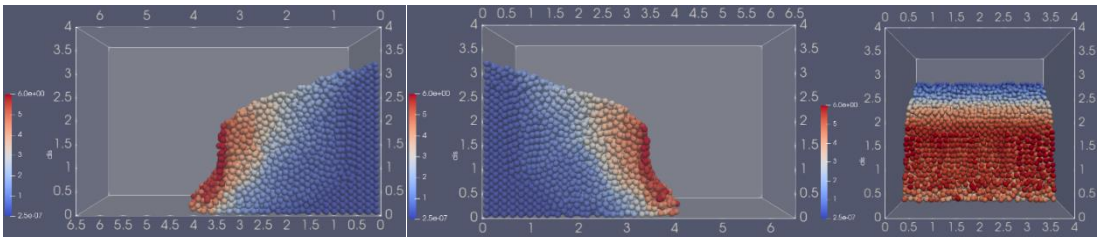

(b) time step=80,000

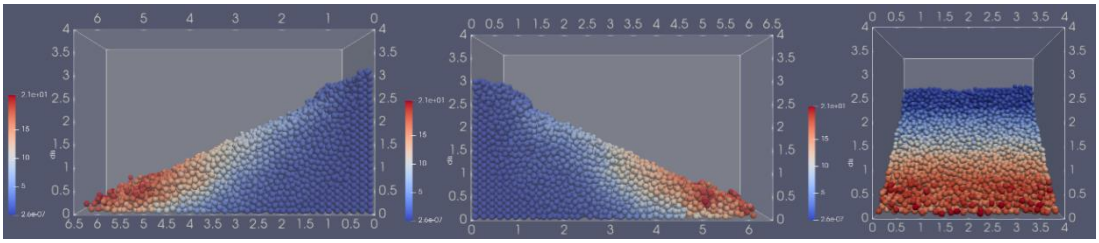

(c) time step=115,000

Fig. 9 Configurations of the initial model and the simulation results at 0, 80,000, 115,000 time steps.

3.3 Test 3

The size of sand column for test 3 is 20*40*60 (length*width*height). Table 4 shows the simulation results with the experimental results and the errors. The displacement results shown in Fig. 10 are basically consistent with the experimental results.

Table 4 Comparison of experimental and simulation results.

	Final deposit height (Hi)	Final deposit length (Li)	Inclination /°
Experiment result	38	92	22
Numerical result	31	83	20.5
Error (%)	18.4	9.8	6.8

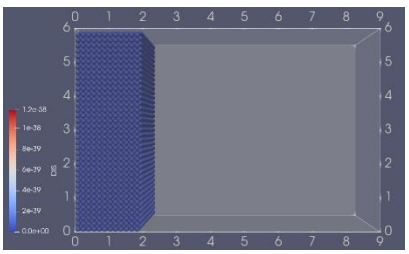

(a) time step=0

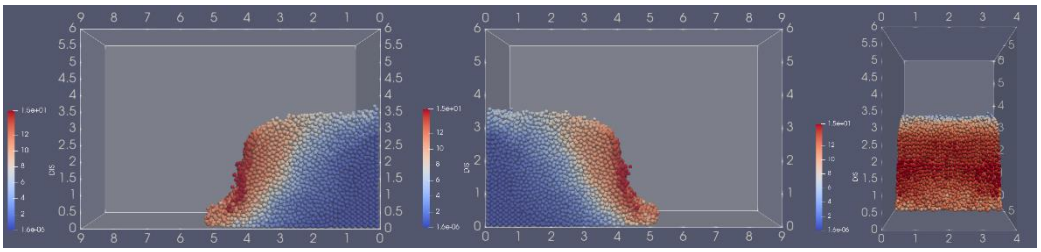

(b) time step=50,000

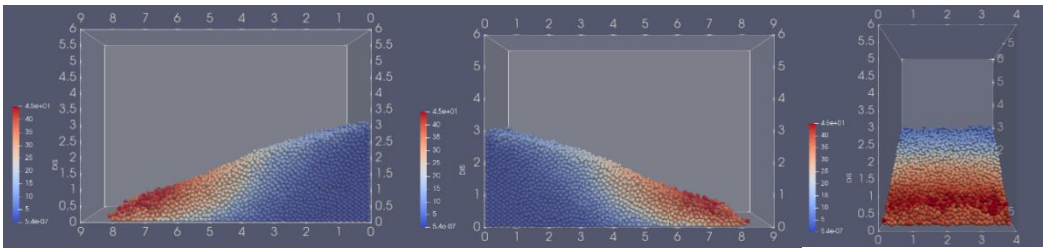

(c) time step=100,000

Fig. 10 Configurations of the initial model and the simulation results at 0, 50,000, 100,000 time steps.

3.4 Test 4

The size of sand column for test 4 is 40*40*20 (length*width*height). Table 5 shows the simulation results with the experimental results and the errors. The displacement results shown in Fig. 11 are basically consistent with the experimental results.

Table 5 Comparison of experimental and simulation results.

	Final deposit height (Hi)	Final deposit length (Li)	Inclination /°
Experiment result	20	65	27
Numerical result	20	75	24
Error (%)	0	15.4	11.11

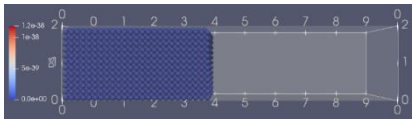

(a) time step=0

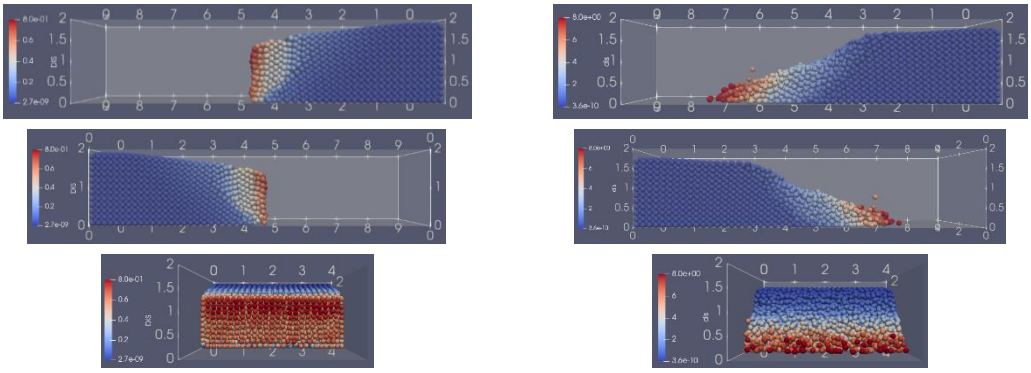

(b) time step=50,000 (c) time step=95,000

Fig. 10 Configurations of the initial model and the simulation results at 0, 50,000, 95,000 time steps.

IV. Prediction results

Based on the calibration results, the parameters in Table 2 of the previous section will be used for simulation to predict the experimental results of Test 5 and 6. The radius of sphere is 0.0069m, and the total number of spheres in each model are: 14412, 21756 respectively.

4.1 Test 5

The size of sand column for test 5 is 20*40*20 (length*width*height) with baffle. The prediction of position results is shown in table 6, and the simulation results are shown in Fig. 12.

Table 6 Numerical result of test 5 with baffle.

	The initial height(H)	The initial length(L)	Distance between baffle 2 and baffle 1(S)	Height of sand at baffle 2	Inclination /°
result	40	20	20	12.5	26.6

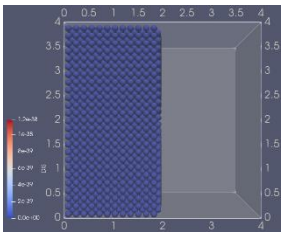

(a) time step=0

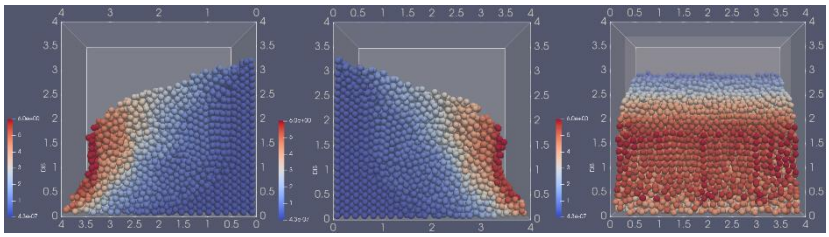

(b) time step=80,000

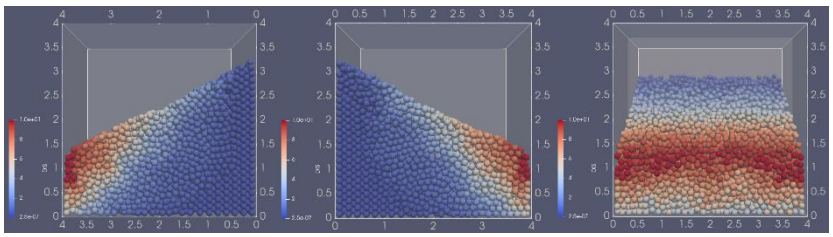

(c) time step=96,000

Fig. 12 Configurations of the initial model and the simulation results at 0, 80,000, 96,000 time steps.

4.2 Test 6

The size of sand column for test 6 is 20*60*20 (length*width*height) with baffle. The prediction of position results is shown in table 7, and the simulation results are shown in Fig. 13.

Table 7 Numerical result of test 6 with baffle.

	The initial height(H)	The initial length(L)	Distance between baffle 2 and baffle 1(S)	Height of sand at baffle 2	Inclination /°
result	40	20	31	14.5	21.9

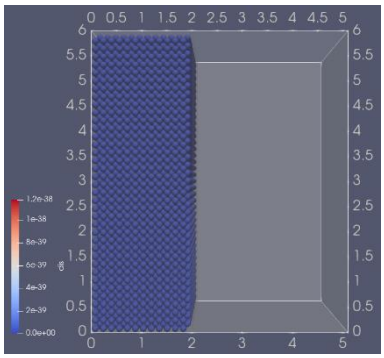

(a) time step=0

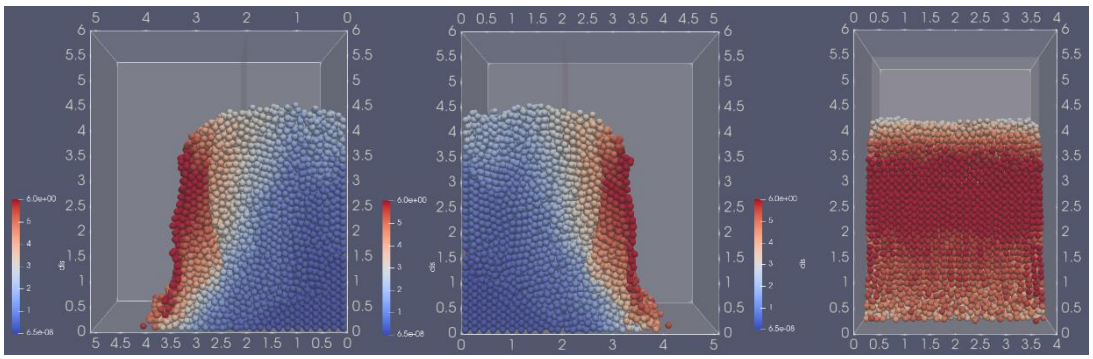

(b) time step=80,000

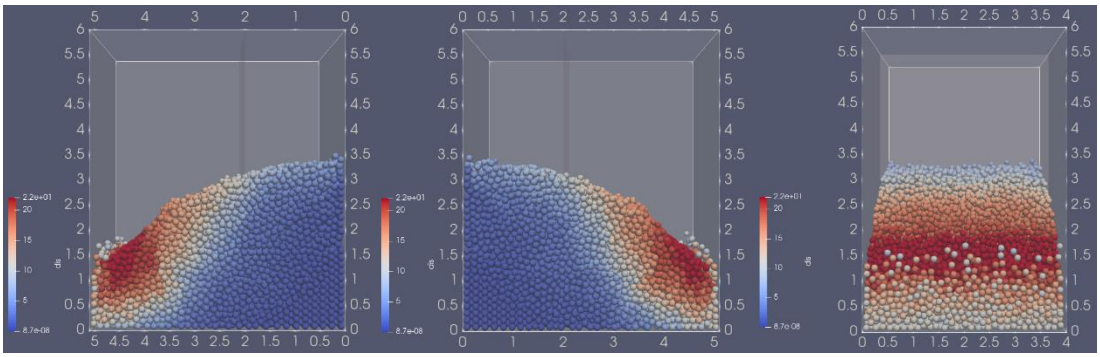

(c) time step=115,000

Fig. 13 Configurations of the initial model and the simulation results at 0, 80,000, 115,000 time steps.

V. Conclusions

The problem B is simulated by self-made 3D SDDA program. The comparison of experiment and simulation results of test 1 to 4 shows the good solving accuracy of 3D SDDA, and the prediction results of test 5 and 6 are obtained. After model 5 was stabilized, the height of the sand column at baffle 2 was 12.5 and the inclination of the slope was 26.6°. After model 6 was stabilized, the height of the sand pile at baffle 2 was 14.5 and the inclination of the slope was 21.9°.

VI. Acknowledgment

References

[1] Jiao Y-Y, Huang GH, Zhao ZY, et al. An improved three-dimensional spherical DDA model for simulating rock failure. Science China Technological Sciences, 2015, 58(9): 1533-1541.

[2] Jiao Y-Y, Wu ZY, Zheng F, et al. Parallelization of spherical discontinuous deformation analysis (SDDA) for geotechnical problems based on cloud computing environment[J]. Science China Technological Sciences, 2021, 64(9): 1971-1980.

[3] Shi G, DDA—a new numerical model for the static and dynamics of block system. 1988, University of California.